MILLER SCALING OF FINGER PROPERTIES IN SANDY SOILS: AN INDIRECT METHOD FOR ESTIMATING FINGER WIDTH AND VELOCITY

R. J. Glass

Geoscience Analysis Division, Sandia National Laboratories, Albuquerque, NM

Laboratory and field experiments have shown infiltration flow instability (or "wetting front instability") to occur in some situations. Wetting front instability is gravity driven and breaks a uniform flat front into vertically moving fingers. Linear stability analysis, dimensional analysis, and experimentation have yielded formulations in two-dimensional systems, for average finger width and velocity as functions of system parameters given by the saturated hydraulic conductivity, K_s, saturated moisture content, sorptivity, initial moisture content, and the flow through the system, q_i. For sandy soils where the Miller scaling theory is appropriate, the theory may be applied to scale finger properties. Miller scaling uses two length scales, one microscopic and the other macroscopic. Nondimensionalizing the flow equations yields scaled forms of the conductivity and moisture characteristics containing the microscopic length scale, m (equivalent to the mean grain size), fluid density, fluid dynamic viscosity, and fluid surface tension. On application to finger properties, one finds the effect on finger width and velocity of soil properties parameterized by m for a family of similar soils. Finger width is found to scale with m while finger velocity scales with $1/m^2$. For q_i/K_s constant, the theory predicts finger width to increase, and finger velocity to decrease, as the soil texture becomes finer. Comparison with data from several preliminary two-layer experiments where the texture of the bottom layer was varied between five similar sands, with m between 1 and 0.125 mm, shows reasonable agreement with the theory.

INTRODUCTION

The subsurface transport of water and contaminants through the vadose zone to an aquifer is important for determining both groundwater recharge and contaminant loading. Many processes influence this transport, some a result of man, others a result of physical properties of the unsaturated zone, weather, and biological activity. While in many situations recharge can be predicted with moderate success, the prediction of contaminant loading has been far less successful. This failure is due in large part to the fact that the flow paths must be known in contaminant transport, while averaged hydraulic properties on the Darcy scale are more useful for modeling the gross movement of water.

The documented high variability of contaminant transport in the field raises the question of cause. Usually, the answer encompasses the spatial variability in hydraulic properties, the presence of cracks/joints/fractures or "macropore flow," and the temporal or spatial variability in water and contaminant supply. In addition to these well known-causes, laboratory and field experiments have shown instability in the flow field itself to occur under some conditions. Figure 1 shows a sequence of two photographs of water infiltrating through a thin two-layer slab of initially dry sand with a fine textured layer overlying a coarse textured bottom layer. As can be seen in the photographs, water moves through "fingers" in the coarse bottom layer as a result of the phenomenon of wetting front instability. When wetting front instability occurs, the flat wetting front moving downward through the unsaturated zone becomes unstable and

breaks into fingers which move vertically to the groundwater, thus by-passing a large portion of the vadose zone. After fingers form, they are found to persist over the course of the infiltration cycle and in subsequent cycles.

It should be obvious that fingering can have a great effect on contaminant transport. Therefore, it is important to determine situations that are unstable so that we can properly model moisture and contaminant transport through the vadose zone. The research problem may be divided into two levels: understanding the basic physics, and applying this basic understanding to field situations. To understand the basic physics, we must determine unstable flow field occurrence and behavior as functions of relevant system parameters, and determine the effect of instability on solute transport. Application to field situations requires documentation of the occurrence of fingers in the field, the development of a screening procedure for determining their occurrence, and the development of monitoring techniques and field scale transport formulations for water and solute where wetting front instability occurs.

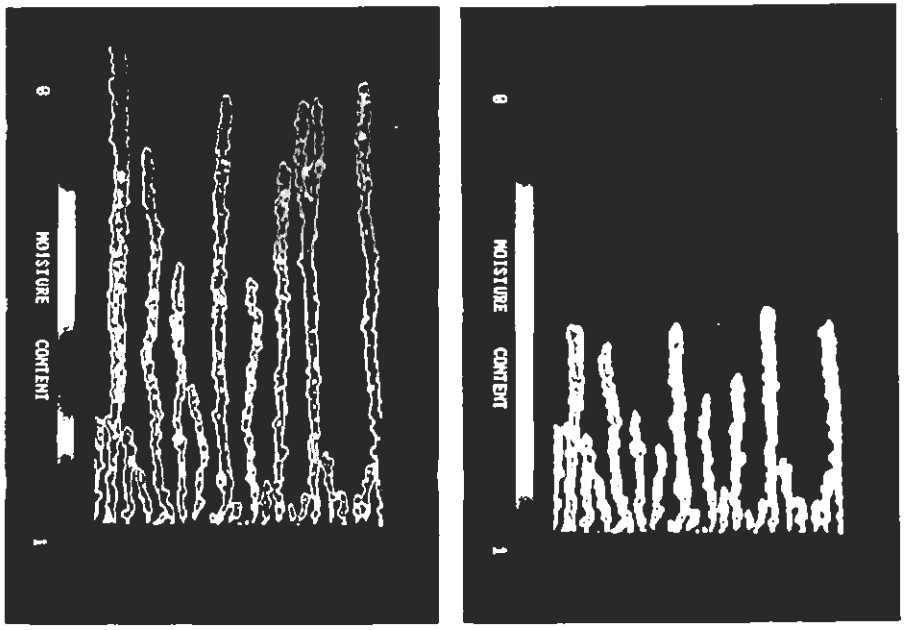

Fig. 1. The downward growth of fingers within an initially dry homogeneous porous medium is shown in a sequence of two images obtained through the use of a new moisture content visualization technique. Infiltration into an unsaturated porous medium can be unstable when the system flux-conductivity ratio, R_p, is less than 1. Water is supplied uniformly to this system at an R_p of 0.1 through a thin top layer of low conductivity (dark rectangular region at top of image). Fingers form directly beneath this uniform supply surface. The medium is 45 cm wide, 76 cm high and 1 cm thick (into the plane of visualization). If the thickness of the medium is less than the minimum finger width, a two-dimensional flow field is forced, as is the case here.

Research on both of these levels has been, and is currently being, conducted by the author along with colleagues at Cornell University, J.-Y. Parlange and T. S. Steenhuis. The emphasis has been on understanding the basic physics of wetting front instability as it defines the importance or relevance of the phenomenon to groundwater hydrology and soil science. In this paper, I will introduce the subject and review recent research that has clarified the basic physics of the fingering process. The review will concentrate on two topics: formulations for finger width and velocity as found through a combination of dimensional analysis, experimentation, and linear stability theory, and the Miller scaling of these relations with a preliminary comparison to data from seven experiments. The application of Miller scaling theory [*Miller and Miller*, 1956] in sandy soils where the theory is appropriate, leads to an indirect method for estimating the finger properties of width and velocity.

BACKGROUND

The stability of the interface between two fluids in a porous medium has been the topic of continuous research in the fields of chemical engineering, fluid mechanics, and petroleum engineering since the discovery of interfacial instability by *Hill* [1952]. The simple heuristic analysis of *Hill* [1952], and the first linear stability analysis of the problem presented by *Saffman and Taylor* [1958] recognize three factors influential in determining the stability of a steady, constant velocity, one-dimensional, vertical downward displacement of one fluid (subscript 2) by another (subscript 1) in a homogeneous, isotropic porous medium: the fluid viscosity difference ($\mu_1 - \mu_2$), the fluid density difference ($\rho_1 - \rho_2$), and the interfacial velocity (U). Their result suggests such a steady, planar displacement is unstable for all wavelengths when the inequality

$$kg(\rho_1 - \rho_2) - \theta_a U(\mu_1 - \mu_2) > 0 \qquad (1)$$

is satisfied (k is the permeability of the media, θ_a is the pore volume available for fluid transport, and g is the gravitational acceleration). While several assumptions have been made to derive this criterion (e.g., the fluids are incompressible, Darcy's law holds for each fluid in the porous media, disturbances are infinitesimal, mixing between the two fluids at the interface is negligible, and θ_a is the same for each fluid), the relationship between buoyant and viscous forces given in (1) is instructive. Flows are seen to be either stabilized or destabilized by viscosity and density differences with the interfacial velocity multiplying the viscosity difference. The role of capillarity at the interface has not been included in the derivation of (1); however, when it is included either through the heuristic approach of *Chouke et al.* [1959] or the more rigorous approach of *Parlange and Hill* [1976], capillary is found to limit the unstable wavelengths to remain above a certain minimum value determined by the properties of the porous medium.

Most research in the field of petroleum engineering has concentrated on viscous-driven instabilities in the absence of gravity, termed "viscous fingering;" a recent review of this literature is given by *Homsy* [1987]. Gravity-driven instabilities in porous media have application to hydrology and soil physics where gravity plays a major role in the movement of water, air, and other fluids, both miscible and immiscible, through the subsurface. In the ubiquitous case of vertical infiltration, a liquid, usually water, moves downward into an air/water filled porous medium. If we assume the velocity of the air/water interface to be constant, the interface to be sharp, and the air to undergo little

compression, then we may apply (1) directly. We see in this case that the density difference is destabilizing while that of viscosity is stabilizing. Because both the viscosity and the density of water is much greater than that of air, (1) simplifies to

$$\theta_a U < \frac{kg\rho_l}{\mu_l} = K_s \tag{2}$$

where K_s is the saturated hydraulic conductivity of the medium. Because $\theta_a U$ is simply the flux through the system, within the constraints of its derivation, (2) predicts that all infiltration flows are unstable when water is supplied at a rate less than the saturated conductivity. Such potentially unstable situations often occur both in the field and in standard laboratory experiments. The case of ponded infiltration into a two-layer system where the top layer is of lower conductivity than the bottom layer, shown in Figure 1, satisfies (2), as does the analogous laboratory experiment where a pressure plate is used to supply water to the top of a uniform soil column. Rainfall or irrigation supplied at a rate less than the saturated conductivity, and redistribution following an infiltration event, may also cause a wetting front to become unstable and fingers to form. In addition to finger formation within unsaturated porous media, identical instabilities should be present in unsaturated fractures/cracks in soil or rock, i.e., in fractures which are supplied with water at a rate less than their saturated conductivity.

While gravity-driven instabilities, or "fingers," were noted in a number of experimental studies within the field of soil physics [e.g., *Palmquist and Johnson*, 1960, 1962; *Tabuchi*, 1961; *Miller and Gardner*, 1962; *Peck*, 1965; and *Smith*, 1967], *Hill and Parlange* [1972] first recognized the application of (2) and conducted a series of experiments to demonstrate the instability of the macroscopic water/air interface when (2) is satisfied. They termed the instability "wetting-front-instability," and the phenomenon has since been the subject of a series of research efforts [e.g., *Raats*, 1973; *Philip*, 1975*a*,*b*; *Parlange and Hill*, 1976; *White et al.*, 1977; *Starr et al.*, 1978, 1986; *Diment et al.*, 1982; *Diment and Watson*, 1983, 1985; *Glass and Steenhuis*, 1984; *Glass et al.*, 1987, 1988*b*; *Tamai et al.*, 1987; and *Hillel and Baker*, 1988].

Beyond the testing of the simple theory resulting in stability criterion (2), a number of interesting facts concerning finger development and unstable flow field behavior have been uncovered through experimentation. The development of fingers, and the steady-state flow field that forms upon long-term ponded infiltration in an initially uniformly dry, fine-over-coarse-textured, layered sand system, was shown qualitatively through the use of dyes and photographic documentation by *Glass and Steenhuis* [1984] and *Glass et al.* [1987, 1988*b*]. Three stages in the evolution of the unstable flow field were noted. The initial stage is dominated by rapid downward movement of fingers that form finger "core" areas. When supplied at a constant flow rate, fully developed fingers maintain a constant finger tip velocity and widen rapidly to a constant width as the finger tip passes. In this stage, relationships among flow through the finger, finger width, and finger velocity, were also discovered. In general, the higher the flow, the wider the finger and the higher the velocity of the finger tip. The second stage is characterized by the persistence of finger core areas that continue to conduct most of the flow, and by the slow lateral movement of lower moisture content wetting fronts from finger core areas into the surrounding dry sand. A less saturated "fringe" area thus develops between the more saturated finger core areas. The lateral movement in the second stage is slow with a time scale on the order of days, while the time scale for downward

finger growth in the first stage is much faster, on the order of minutes. The final stage is a steady-state flow field in which core and fringe areas coexist for long periods of steady infiltration. The second and last phases, which had not been noted by earlier experimental studies, both demonstrate the important feature of core/fringe structure formation.

In addition to demonstrating the formation of the core/fringe structure during steady infiltration events, *Glass and Steenhuis* [1984] and *Glass et al.* [1987, 1988*b*] demonstrated the persistence of fingers from one infiltration cycle to the next. After an interruption in the water supply, and drainage to field capacity, fingers form in the same locations as they did in the first cycle and have the same core areas, which continue to conduct almost all water. Fringe area contribution is higher than in the first cycle, and a steady-state flow field is achieved much more rapidly. If the chamber is flooded and drained so that the initial moisture content field is made uniform, core areas are obliterated, thus emphasizing that finger persistence was not caused by heterogeneities in the porous material, either in the initial pack or because of possible reorientation of grains by the initial fingers themselves.

While the dramatic core and fringe structure has not yet been demonstrated to occur in uniformly wet sands near field capacity, infiltration with such an initial condition appears to be unstable at a wavelength an order of magnitude longer than in the initially dry sand. Because this wavelength was on the order of the chamber width in these experiments, the instability of wet systems has not yet been unambiguously determined. However, instability at a longer wavelength was indicated by the study of *Diment and Watson* [1985] in sands wet below field capacity.

While fingers are difficult to observe in the field, the use of dyes as tracers by *Starr et al.* [1978] and *Glass et al.* [1988*b*] have shown finger structures to occur in two fine-over-coarse layer systems under initially wet conditions (river valley in Connecticut and Long Island, New York). Based upon the discovery of finger persistence in the laboratory, the fingers illuminated by the dyes in both of these studies were most likely persisting finger channels and would have been extremely difficult to detect using traditional field moisture measurement techniques. Other field experiments conducted in the Netherlands by *Hendrickx et al.* [1988], *van Ommen and Dijksma* [1988], and *van Ommen et al.* [1988] have also demonstrated the occurrence of fingers under field conditions.

REVIEW OF RECENT RESEARCH

Formulations for Finger Properties: Width and Velocity

To further clarify the basic physics of fingering, a theoretical framework for systematic wetting front instability experimentation is developed through classical dimensional analysis [*Glass et al.*, 1989*b*]. Nondimensionalization of the diffusion form of Richards' equation, using the sorptivity, S, to scale the soil water diffusivity and K_s to scale the hydraulic conductivity, yields the dimensionless parameter N defined as

$$N = \frac{dk_s(\theta_s - \theta_i)}{S^2} \tag{3}$$

where d is the finger width, θ_s and θ_i are the saturated and initial moisture contents respectively, and S is evaluated between θ_i and θ_s at a pressure head of ψ_{wf}, the effective

water entry value. N expresses the ratio of gravity to capillary forces. Through dimensional analysis at the finger-scale, finger width, d, in an isotropic and homogeneous porous media is shown to be

$$d = \frac{S^2}{(\theta_s - \theta_i)K_s} f_{dF}(R_F) \tag{4}$$

where $f_{dF}(R_F)$ must be provided through experimentation. The dimensionless flux-conductivity ratio, R_F, brings in the boundary condition and is given by

$$R_F = q_f / K_s \tag{5}$$

where q_F is the flux into the finger defined by the flow rate through the finger divided by the cross-sectional area of the finger. Finger propagation velocity, v, is also a function of R_F given as

$$v = \frac{K_s}{\theta_s - \theta_i} f_{vF}(R_F) \tag{6}$$

where the function $f_{vF}(R_F)$ must again be provided through experimentation.

The same analysis may be applied to the larger chamber-scale of a two-layer system by replacing the average flux into a finger, q_F, by the average flux into the entire system, q_S, defined by the flow rate through the system divided by the cross-sectional area of the system. Instead of R_F at the chamber scale, the dimensionless group R_S is defined

$$R_S = q_S / K_s \tag{7}$$

resulting in

$$D = \frac{S^2}{(\theta_s - \theta_i)K_s} f_{dS}(R_S) \tag{8}$$

and

$$V = \frac{K_s}{(\theta_s - \theta_i)} f_{vS}(R_S) \tag{9}$$

where D and V denote chamber scale averages, whereas $f_{dS}(R_S)$ and $f_{vS}(R_S)$ must be determined experimentally. Note that R_S and R_F can be related by

$$R_F = \beta R_S \tag{10}$$

where R_F is defined using the average flux through the fingers that form in the chamber. β is simply the reciprocal of the fractional cross-sectional area containing fingers; this parameter will be a function of R_F.

In *Glass et al.* (1989c), the results of experiments that determine $f_{dF}(R_F)$, $f_{vF}(R_F)$, $f_{dS}(R_S)$ and $f_{vS}(R_S)$ are presented for two-dimensional, unstable flow fields that develop in initially dry, fine-over-coarse, layered sand systems. Equations (4) and (6) become

$$d = \frac{S^2}{K_s(\theta_s - \theta_i)} \frac{3}{(1 - R_F)} \tag{11}$$

and

$$v = \frac{K_s}{(\theta_s - \theta_i)}[C_2 + R_F(1 - C_2)] \tag{12}$$

where C_2 is a constant found empirically to be 0.1. Because fingers are not fully saturated as assumed by *Parlange and Hill* [1976] (they move at different velocities), their analysis may be repeated without this restriction. Linear stability theory then yields

$$D = \frac{\pi S^2}{K_s(\theta_s - \theta_i)} \frac{1}{(1 - q_S / q_F)} \tag{13}$$

where K_F is the value of K at θ_F, the moisture content of the finger. Comparison of the theory with experimental results yields $\beta = 1/R_F$ and thus we have for average finger properties

$$D = \frac{\pi S^2}{K_s(\theta_s - \theta_i)} \frac{1}{(1 - R_S^{1/2})} \tag{14}$$

and

$$V = \frac{K_s}{(\theta_s - \theta_i)}[C_2 + R_S^{1/2}(1 - C_2)] \tag{15}$$

At the chamber scale, V is equally well represented with C_2 equal to zero as to 0.1. Because a zero value allows the more physical result of zero velocity for zero flow, we take C_2 equal to zero in (15) for V in the remainder of the paper.

Miller Scaling of Finger Properties

Equations for finger width and velocity may be extended through the concept of similar porous media flow systems [*Glass et al.*, 1989*b*]. This study shows explicitly the effect of the mean grain size and fluid surface tension, viscosity, and density on finger width and velocity for a family of similar porous media. The concept of similarity between two porous media flow systems demands that the functional forms of $K(\theta)$ and $\psi(\theta)$ be identical with their scale factors incorporated into N, the gravity-capillarity ratio. Therefore, relationships derived between N and R_F or R_S from dimensional analysis are expected to apply to two porous media where these forms are the same.

The functional forms of $K(\theta)$ and $\psi(\theta)$ depend on pore-size distribution, shape, and connectivity. Grain size distributions that scale logarithmically and are packed to the same bulk density, are "similar" in the sense of *Miller and Miller* [1956]. Miller scaling uses two length scales, one microscopic and the other macroscopic. Nondimensionalizing the flow equations yields scaled forms of the conductivity and moisture characteristics containing the microscopic length scale, m (equivalent to the mean grain size), fluid density, ρ, fluid dynamic viscosity, μ, and fluid surface tension, σ. Application to our system parameters yields

$$K_s = \frac{\rho g m^2}{\mu} K_{s*} \tag{16}$$

$$S^2 = \frac{\sigma m}{\mu} S_*^2 \tag{17}$$

$$R_F = \frac{\mu}{\rho g m^2} \frac{q_F}{K_{s*}} \tag{18}$$

and

$$N = \frac{m \rho g}{\sigma} \frac{dK_{s*}(\theta_s - \theta_i)}{S_*^2} \tag{19}$$

where K_{s*} and S_*^2 are dimensionless. The scaling of N and R_F shows that d will scale by $1/m$ and q_F by m^2, so that dm and q_F/m^2 must be the same for similar flow behavior. Equation (11) may be written more generally as

$$d = \frac{\sigma}{\rho g m} \frac{\pi S_*^2}{K_{s*}(\theta_s - \theta_i)} \frac{1}{(1 - R_F)} \tag{20}$$

Equation (20) states that for a family of similar sands, and q_F chosen such that q_F/m^2 is a constant, the product of d and m is a constant; that is, as m decreases, fingers will be wider. The velocity may also be scaled yielding

$$v = \frac{\rho g m^2}{\mu} \frac{K_{s*}}{(\theta_s - \theta_i)} [C_2 + R_F(1 - C_2)] \tag{21}$$

Equation (21) shows the velocity scale by m^2 so that, for q_F/m^2 a constant, the ratio of v to m^2 is also a constant.

In the Miller scaled form, the effects of σ, ρ, and μ also are seen on finger size and velocity. An increase in the ratio σ/ρ will decrease N and increase the finger width for a given R_F. The ratio μ/ρ, which is defined as the dynamic viscosity, affects the variable R_F such that for $m^2 R_F$ a constant, $q_F \mu/\rho$ must be the same.

At the chamber scale we have similarly

$$D = \frac{\sigma}{\rho g m} \frac{\pi S_*^2}{K_{s*}(\theta_s - \theta_i)} \frac{1}{(1 - R_S^{1/2})} \tag{22}$$

and

$$V = \frac{\rho g m^2}{\mu} \frac{K_{s*}}{(\theta_s - \theta_i)} R_S^{1/2} \tag{23}$$

where R_S is scaled similarly to R_F.

Several experiments have been conducted on sands similar to the sand used by *Glass et al.* [1989*b*] to quantify (12), (13), (14), and (15) (m = 0.0991 cm, US sieve series 14-20 fraction). The Miller scaled forms may be tested through a comparison with these experiments; however, because these experiments were conducted as the techniques were being developed, the results of this comparison to theory must be considered to be preliminary. Figures 2 and 3 show a plot of d and v versus $R_S^{1/2}$ for the five values of m (0.0991, 0.0707, 0.337, 0.210, and 0.0125 cm) encompassed by the experiments. Table 1 contains the pertinent data for the comparison. It can be seen that the finger widths, predicted with (22), are 37.5 and 35 for Experiments 6 and 7, respectively. Because these widths are larger than the width of the chamber (30 cm), fingers cannot form and the flow field should remain stable, which was the case in these experiments. For Experiments 1 through 5, we may most easily compare predicted properties with measured properties by writing

$$D_* = \frac{\rho g m}{\sigma} D \tag{24}$$

and

$$V_* = \frac{\mu}{\rho g m^2} V \tag{25}$$

so that all the curves in Figures 2 and 3 collapse into one.

TABLE 1. Data from Preliminary Two-Layer Experiments

Exp #	m (cm)	R_S	D (cm)	V (cm/min)
1	0.0707	0.05	2.3	15.2
2	0.0337	0.07	4	4
3	0.0337	0.37	12.7	9
4	0.0337	0.95	20.7	11.8
5	0.0210	0.19	10	2.3
6	0.0210	0.72	-†	-†
7	0.0125	0.54	-†	-†

† stable wetting front

The functional forms of $K(\theta)$ and $\psi(\theta)$ depend on pore-size distribution, shape, and connectivity. Grain size distributions that scale logarithmically and are packed to the same bulk density, are "similar" in the sense of *Miller and Miller* [1956]. Miller scaling uses two length scales, one microscopic and the other macroscopic. Nondimensionalizing the flow equations yields scaled forms of the conductivity and moisture characteristics containing the microscopic length scale, m (equivalent to the mean grain size), fluid density, ρ, fluid dynamic viscosity, μ, and fluid surface tension, σ. Application to our system parameters yields

$$K_s = \frac{\rho g m^2}{\mu} K_{s*} \tag{16}$$

$$S^2 = \frac{\sigma m}{\mu} S_*^2 \tag{17}$$

$$R_F = \frac{\mu}{\rho g m^2} \frac{q_F}{K_{s*}} \tag{18}$$

and

$$N = \frac{m \rho g}{\sigma} \frac{dK_{s*}(\theta_s - \theta_i)}{S_*^2} \tag{19}$$

where K_{s*} and S_*^2 are dimensionless. The scaling of N and R_F shows that d will scale by $1/m$ and q_F by m^2, so that dm and q_F/m^2 must be the same for similar flow behavior. Equation (11) may be written more generally as

$$d = \frac{\sigma}{\rho g m} \frac{\pi S_*^2}{K_{s*}(\theta_s - \theta_i)} \frac{1}{(1 - R_F)} \tag{20}$$

Equation (20) states that for a family of similar sands, and q_F chosen such that q_F/m^2 is a constant, the product of d and m is a constant; that is, as m decreases, fingers will be wider. The velocity may also be scaled yielding

$$v = \frac{\rho g m^2}{\mu} \frac{K_{s*}}{(\theta_s - \theta_i)} [C_2 + R_F(1 - C_2)] \tag{21}$$

Equation (21) shows the velocity scale by m^2 so that, for q_F/m^2 a constant, the ratio of v to m^2 is also a constant.

In the Miller scaled form, the effects of σ, ρ, and μ also are seen on finger size and velocity. An increase in the ratio σ/ρ will decrease N and increase the finger width for a given R_F. The ratio μ/ρ, which is defined as the dynamic viscosity, affects the variable R_F such that for $m^2 R_F$ a constant, $q_F \mu/\rho$ must be the same.

At the chamber scale we have similarly

$$D = \frac{\sigma}{\rho g m} \frac{\pi S_*^2}{K_{s*}(\theta_s - \theta_i)} \frac{1}{(1 - R_S^{1/2})} \tag{22}$$

and

$$V = \frac{\rho g m^2}{\mu} \frac{K_{s*}}{(\theta_s - \theta_i)} R_S^{1/2} \tag{23}$$

where R_S is scaled similarly to R_F.

Several experiments have been conducted on sands similar to the sand used by *Glass et al.* [1989*b*] to quantify (12), (13), (14), and (15) (m = 0.0991 cm, US sieve series 14-20 fraction). The Miller scaled forms may be tested through a comparison with these experiments; however, because these experiments were conducted as the techniques were being developed, the results of this comparison to theory must be considered to be preliminary. Figures 2 and 3 show a plot of d and v versus $R_S^{1/2}$ for the five values of m (0.0991, 0.0707, 0.337, 0.210, and 0.0125 cm) encompassed by the experiments. Table 1 contains the pertinent data for the comparison. It can be seen that the finger widths, predicted with (22), are 37.5 and 35 for Experiments 6 and 7, respectively. Because these widths are larger than the width of the chamber (30 cm), fingers cannot form and the flow field should remain stable, which was the case in these experiments. For Experiments 1 through 5, we may most easily compare predicted properties with measured properties by writing

$$D_* = \frac{\rho g m}{\sigma} D \tag{24}$$

and

$$V_* = \frac{\mu}{\rho g m^2} V \tag{25}$$

so that all the curves in Figures 2 and 3 collapse into one.

TABLE 1. Data from Preliminary Two-Layer Experiments

Exp #	m (cm)	R_S	D (cm)	V (cm/min)
1	0.0707	0.05	2.3	15.2
2	0.0337	0.07	4	4
3	0.0337	0.37	12.7	9
4	0.0337	0.95	20.7	11.8
5	0.0210	0.19	10	2.3
6	0.0210	0.72	-†	-†
7	0.0125	0.54	-†	-†

† stable wetting front